Available online at www.sciencedirect.com
ScienceDirect
Thermochimica Acta 456 (2007) 128–133
thermochimica acta
www.elsevier.com/locate/tca

Thermogravimetric study of some crosslinked copolymers based on poly(acrylonitrile-*co*-divinylbenzene)

E.C. Riqueza[a], A.P. de Aguiar[a,*], M.R.M.P. de Aguiar[b], L.C. de Santa Maria[b,*]

[a] *Departamento de Engenharia Química, Instituto Militar de Engenharia, Praça General Tibúrcio, 80 Rio de Janeiro, RJ 22290-270, Brazil*
[b] *Instituto de Química, Universidade do Estado do Rio de Janeiro, R. São Francisco Xavier, 524 Rio de Janeiro, RJ 20559-900, Brazil*

Received 20 June 2006; received in revised form 4 February 2007; accepted 20 February 2007
Available online 27 February 2007

Abstract

Copolymer networks based on acrylonitrile (AN)/divinylbenzene (DVB) have been investigated by thermogravimetric analysis (TG) to evaluate their thermal stability in nitrogen atmosphere. Thermal stability was determined from TG-DTG curves to investigate the influence of AN and DVB in the synthesis of copolymers on the copolymer thermal properties. The TG and DTG curves of copolymers clearly show two thermodegradation stages. The solid residues produced after thermodegradation stages were analyzed by FTIR and elemental analysis (CHN). The decomposition temperatures were dependent on amount of AN and DVB used as the crosslinking agent. The degradation temperatures of copolymers were influenced by the diluent system during their synthesis. FTIR analyses indicate that the cyclization of the polymer proceeds before any mass loss.

Keywords: Thermal stability; Thermogravimetry; Poly(acrylonitrile-*co*-divinylbenzene)

1. Introduction

Copolymer networks with controlled porous structure are widely employed as starting materials for ion exchangers, as specific sorbents, as packing for gel permeation chromatography and as catalyst support [1–4]. The morphological control of the copolymer beads and their porous structures may result in many advantages concerning removal of metal ions and other pollutants from wastewater. These characteristics have a strong influence on the removal kinetics and flow properties [2].

Crosslinked copolymers based on acrylonitrile (AN) have a great potential for many applications as chelating resins, catalyst supports, in the water purification industry, in monitoring heavy metals, and as other useful materials [5–7]. However, there are very few papers about thermogravimetric study of AN crosslinked with divinylbenzene (DVB) [8–10].

Some papers present study about thermal degradation (thermal resistance, mechanisms of thermolysis and thermooxidation) of polymers (including copolymers with monofunctional monomers) based on acrylonitrile. For carbon fiber production, polyacrylonitrile (PAN) are stabilized by heating in air at temperatures in the range 200–300 °C, prior to carbonization in an inert atmosphere at temperatures above 1000 °C [8,11].

Literature has pointed out various reactions during thermal treatment of polymers based on AN [12–17]. The formation of a heteroaromatic structure was suggested [18]. Afterward cyclic polyimine structures (frequently referred to as “ladder polymer”) are favored, which may undertake tautomerization to a polyenamine, followed by isomerization [19] and supplementary reactions [20]. Many researchers believe that the initial step in the degradation is an intramolecular cyclization [20,21]. Other authors propose that the cyclization reaction occurs by nucleophilic attack on the nitrile groups [19].

Some researchers have also suggested that various types of intermolecular crosslinking may take place [22] or that dehydrogenation may result in conjugated polyenes [23]. Ferguson and Mahapatro suggested that oxidative chain degradations also participate with cyclization [24]. The production of HCN on thermal oxidative degradation at temperatures above 250 °C was attributed to a process of chain scission [25].

The purpose of the present work was a thermogravimetric study for poly(acrylonitrile-*co*-divinylbenzene) prepared with different AN/DVB molar relations and diverse porosities.

---

[*] Corresponding authors. Tel.: +55 21 2546 7080; fax: +55 21 2546 7059.
E-mail addresses: alcino@ime.eb.br (A.P. de Aguiar), santamaria@pesquisador.cnpq.br, lcsantamaria@terra.com.br (L.C. de Santa Maria).

0040-6031/$ – see front matter © 2007 Elsevier B.V. All rights reserved.
doi:10.1016/j.tca.2007.02.014

Table 1
Synthesis parameters of copolymer networks

Resin	Diluent system (%)	Feed monomers (mol%) AN/DVB	Yield (%)
R1	100ANI	60/40	65
R2	70ANI/30HEP	60/40	60
R3	100ANI	80/20	75
R4*	100ANI	80/20	82
R5	70ANI/30HEP	80/20	74
R6	65ACT/35TOL	80/20	85

Polymerization conditions: aqueous phase (AP) composed of gelatin and 2-hydroxyethyl-celullose (both suspension stabilizers at 0.3 wt.% with respect to the AP) and Na_3PO_4 (2 wt.% in relation to AP) or *NaCl (2 wt.% in relation to AP); AIBN used as initiator (1.0 mol% with respect to the monomers); dilution degree = 150% (dilution in relation to total volume of monomers); HEP = *n*-heptane, TOL = toluene, ACT = ethyl acetate, ANI = anisole, AN = acrylonitrile and DVB = divinylbenzene.

2. Experimental

2.1. Materials

Commercial DVB (grade of 45% of DVB, containing a mixture of DVB and ethylvinylbenzene) and AN were kindly donated by Nitriflex (Brazilian Co.) and used as received. α,α'-Azo-bis-isobutyronitrile (AIBN, donated by Metacril, Brazilian Co.) was purified by recrystallization from methanol. 2-Hydroxyethyl-cellulose (HEC, Cellosize QP-100 MH) was donated by Union Carbide and used as received. The other reagents were commercially purchased, namely gelatin, propanone, methanol, NaCl, Na_3PO_4, *n*-heptane (HEP), anisole (ANI), ethyl acetate (ACT), toluene (TOL) (Vetec Química Fina Ltda, Brazil) with P.A. degree and used as received. Aqueous solutions were prepared using distilled deionized water.

AN and DVB copolymerizations were carried out as described elsewhere [6]. The synthesis parameters of AN/DVB copolymers were summarized in Table 1. These copolymers were obtained in a typical glass reactor (1000 mL) fitted with mechanical stirrer using the aqueous suspension polymerization technique. Aqueous phase (AP) was composed by gelatin and 2-hydroxyethyl-celullose (both at 0.3 wt.% with respect to AP) and Na_3PO_4 (2 wt.% in relation to AP) or NaCl (2 wt.% in relation to AP). The organic phase (OP) was composed by monomers mixture (monomers, diluent system at dilution of 150% (v/v) in relation to the monomers) and AIBN used as initiator (1.0 mol% with respect to the monomers). OP was added slowly to AP previously prepared under stirring at room temperature, employing AP/OP ratio = 3/1. These two phases were maintained under stirring (300 rpm) at room temperature for 10 min. Then, the suspension copolymerization system was kept under stirring at 70 °C for 24 h. The resin beads were thoroughly washed with hot water (8 portions of 500 mL), extracted with propanone (Soxhlet extractor) and dried around 90 °C. The diameter of obtained beads was around 50–100 μm.

2.2. Characterization

The copolymers were analyzed by Fourier transform infrared spectrometer (FTIR-Perkin Elmer mod. 1710×) using KBr pellets. The TG and DTG analyses were carried out with powdered resin beads. The copolymers porous structure was characterized earlier [6].

Thermal analyses of copolymers were conducted with a Shimadzu TG-50 at a heating rate of 10 °C min^{-1} under nitrogen (99.99% purity) with a platinum pan at temperatures from ambient (∼25 °C) to 800 °C. The powdered sample, about 5 mg in weight was packed into the platinum pan and the gas flow rate was kept at 30 mL min^{-1}.

The beads porosity was determined by BET or BJH methods from low-temperature nitrogen adsorption isotherms (ASAP Micromeritics 2010), which were obtained at 77 K using a high-vacuum volumetric apparatus. The samples were degassed at 100 °C/1 mPa for 3 h.

Copolymer beads were also characterized at a scanning electron microscope (SEM, JEOL JSM–5800LV apparatus). The beads were coated with gold by sputtering. Their external and internal parts were observed using 10 kV acceleration electron beam.

3. Results and discussions

Table 2 shows the characteristics of AN/DVB resins. Their N contents evidence the AN incorporation in the copolymers. In earlier results, we had observed that the AN incorporation and the copolymer porosity are related to the solubility parameter and the dielectric constant of diluent employed in the copolymer synthesis [5,6]. The highest AN incorporation was attained for the R6 resin compared to those prepared with the same AN amount added to the feed (namely, R3, R4 and R5 resins). These results could be explained by the different dielectric constants (ε) of the diluents employed in the copolymer synthesis. Therefore, it seems that the diluent polarity has an important role on the AN incorporation due to the solvation capacity, consequently minimizing its solubility in water [5].

In addition, the reactivity ratios for the monomers present in the system composed by AN (monomer 1) and commercial DVB [mixture of *m*-DVB (monomer 2) and *p*-DVB (monomer 3)] are $r_{31} = 4.52$, $r_{13} = 0.20$, $r_{21} = 1.55$, $r_{12} = 0.26$, $r_{32} = 1.55$ and $r_{23} = 0.42$. These values point out that the AN-DVB copolymer produced at the initial stages is more loaded with DVB units than the monomer mixture and therefore there is a trend to form

Table 2
Chemical analysis and specific surface area of copolymer networks

Resin	(g/mL)[a]	V_p (cm^3/g)[b]	D_p (Å)[c]	S (m^2/g)[d]
R1	0.4	0.32	70	184
R2	0.2	0.54	118	232
R3	0.4	0.56	141	126
R4	0.4	0.43	249	70
R5	0.2	0.32	202	63
R6	0.3	0.44	222	72

Elemental analysis (CHN), error = 0.1%.

[a] Apparent density.

[b] Average pore diameter determined by BJH method.

[c] Average pore volume determined by BJH method.

[d] Specific surface area determined by BET method.

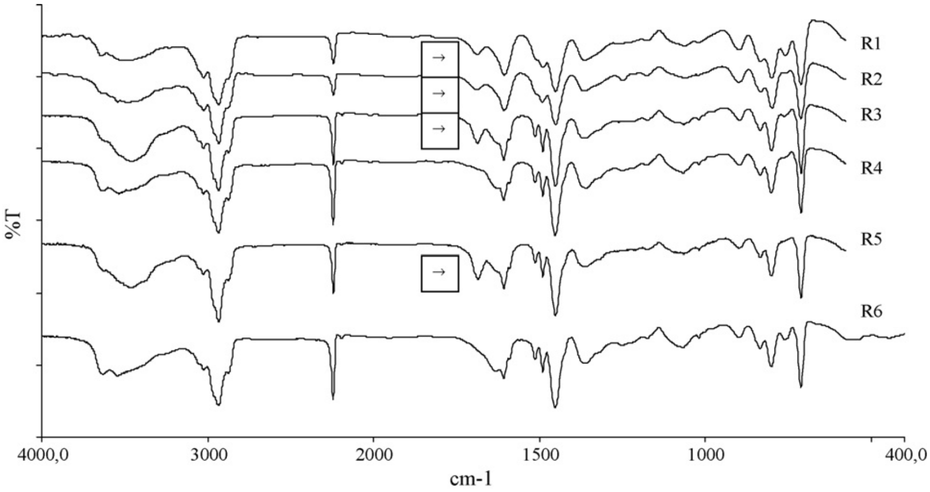

Fig. 1. FTIR spectra of the copolymers based on acrylonitrile and divinylbenzene.

microgels (phase separation). However, whereas the microgels are well solvated by aromatic monomers, the AN monomer is a poor solvent. Therefore, if the larger is the fraction of AN in the system, the earlier the phase separation or precipitation of microgels occurs [26–30].

We can observe that when the AN amount in the feed was increased the inhomogeneity of polymeric network was also increased due to the poor solvation conditions for the involved monomers or formed polymer [4,31]. The S, D_p and V_p data (Table 2) show that the copolymer porosity was dependent on the AN content, and on the diluent system employed (Table 1) in their synthesis. By the results of apparent density (D_a) and porosity (S, D_p and V_p values in Table 2), we can clearly note that the ANI was a better solvent for the AN/DVB monomer system. This solvent produced copolymer with higher D_a and smaller pores compared to the others ones.

FTIR spectra of all copolymers have an absorption band at 2240 cm^{-1} attributed to CN stretching vibration of the AN units, confirming the AN incorporation [20,32,33]. Fig. 1 shows typical spectra of copolymers. The R1, R2, R3 and R5 spectra show the absorption at 1720–1670 cm^{-1} indicated with arrows. This absorption could be attributed to carboxyl groups from amide or carboxylate (C=O stretching vibration). The carbonyl appearance might be produced by the alkaline hydrolysis of nitrile groups due to the Na_3PO_4 use in aqueous phase (pH 12–13). This way, higher pH conditions (pH 12) were expected to be the responsible for the production of hydrolyzed material [20]. For confirming this goal, the R4 resin was synthesized using NaCl in the aqueous phase (pH around 7). As it can be seen in Fig. 1, the carboxyl band absorption was not displayed on the R4 spectrum.

By analyzing Figs. 2 and 3, it can be possible to notice that the competing processes of destruction and crosslinking could accompany the pyrolysis of a polymeric material. The predominance of the destruction process leads to the full disintegration of the initial material to monomers (depolymerization process) and simple compounds, and to a carbon frame representing the carbonized product (raw carbon). The main chemical processes involved are dehydration and dehydrogenation, the removal of low molecular compounds of hydrogen with carbon and heteroatoms, oxidation, and the linkage of fragments of polymeric chains with the formation of polynuclear structure involving the adjacent nitrile units with the elimination of ammonia [20,34]. Since the number of neighboring nitriles in random polymers should be big due the larger AN amounts employed for the syn-

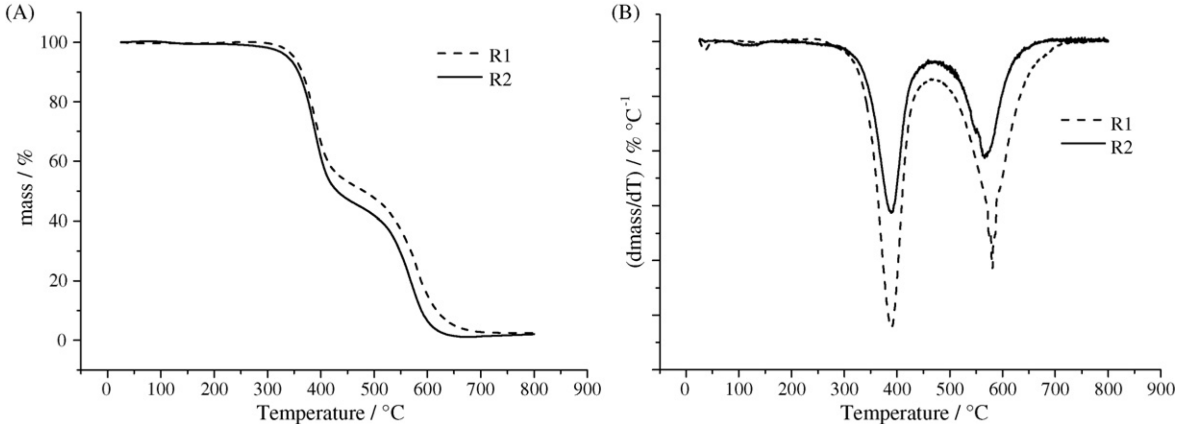

Fig. 2. TG (A) and DTG (B) curves of the AN/DVB copolymers (R1 and R2 resins) under nitrogen at a heating rate of 10 °C min^{-1}.

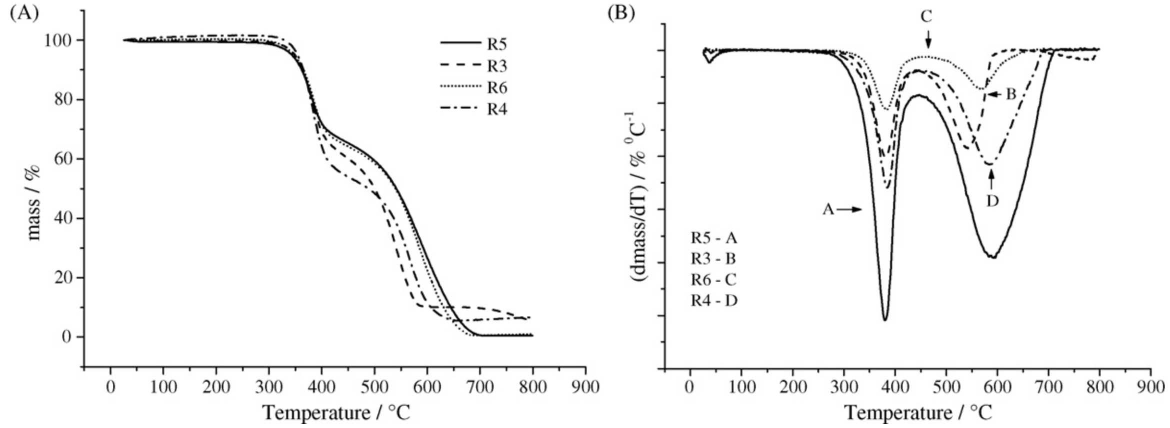

Fig. 3. TG (A) and DTG (B) curves of the AN/DVB copolymers (R3, R4, R5 and R6 resins) under nitrogen at a heating rate of 10 °C min^{-1}.

thesis of R3, R4, R5 and R6 resins (see Table 1), this supports the suggested degradation pathway of this polynuclear structure arrangement.

Generally, the TG and DTG curves (Figs. 2 and 3) show that all copolymers are thermodegraded in two stages and nearly crumbled between 600–700 °C (char yield around 2%). This result evidence that the almost all polymer mass was crumbled in gaseous products. The earlier process relates to the elimination of moisture (around 110 °C). The first stage of sharp loss in mass (T_{dm1} around 379–390 °C, see Table 3) is mostly attributed to the DVB degradation (T_{onset} around 347–353 °C). Considering the aromatic component, the appearance of degradation products (benzene, toluene and styrene monomer and oligomers) begins at about 347 °C could be attributed to DVB units. These are most likely connected with the polycondensation of aromatic chains [34]. This mass loss seems to be related to the crosslinking degree. One observes that the copolymers with larger DVB content (R1 and R2) present higher T_{dm1} compared to those with lower DVB contents (R3, R4, R5 and R6). For a polymeric matrix based on AN, the main loss in mass takes place in the temperature interval of 250–600 °C (Table 3), and the major products of pyrolysis are HCN and NH_3 [20,34]. Above 600 °C, molecular hydrogen is among the main products (low loss in mass). The least stable stage (T_{dm2}, see Table 3) may be due to the most stable step related to the random scissions process from uncyclized segments of AN units. This process could be confirmed by the FTIR spectra of the polymer residues shown in Fig. 4. The spectra display absorption bands attributed to C=C (1590–1670 cm^{-1}) and C=N (1580–1620 cm^{-1}) [20,32,34].

Table 3
Thermal decomposition temperatures of the modified copolymers

Resin	T_{dm1}[a] (°C) (±3 °C)	Total weight loss (%)	T_{dm2}[a] (°C) (±3 °C)	Total weight loss (%)
R1	390	47	581	50
R2	388	53	566	45
R3	381	40	542	54
R4	380	35	591	64
R5	379	47	558	50
R6	384	36	584	62

[a] T_{dm} = temperature at the maximum weight-loss rate.

These residues proceeding from the degradation in 450 and 600 °C of the R3 copolymer had been analyzed by FTIR and elemental analyses (CHN). Fig. 4 shows the spectra of the original copolymer (R3) and its residues. The CHN values of the original copolymer and its residue at 450 °C are shown in Table 4.

The FTIR spectra of Fig. 4 evidence the gradual but significant reduction of the CN band at 2240 cm^{-1}. This reduction can be explained by cyclization process of the repetitive AN units promoted by the thermolysis process, leading to the polyimine/enamine structures, which display the broad band at 1585 cm^{-1} [16]. In addition, the residue at 450 °C has presented a shoulder at 1712 cm^{-1}, which could be attributed to C=O from carboxylic groups formed by the thermooxidation of AN groups. This spectrum also displayed a strong absorption at 1596 cm^{-1}, which could be assigned to C=C (1590–1670 cm^{-1}) and C=N (1580–1620 cm^{-1}).

The results of elemental analysis of R3 and its residue show that after the thermodegradation at 450 °C, the oxygen content has increased. This results point out the generation of thermooxidation products, confirming the FTIR observations. The degradation products of polymers based on acrylonitrile at temperatures below 400 °C normally are NH_3, HCN and H_2O [20]. Hence, the significant reduction in nitrogen and hydrogen contents (Table 4) can be attributed to the release of these substances.

The FTIR spectra (Fig. 4) of the R3 residues obtained at 450 and 600 °C in TGA experiments are different from that of the starting material as new bands appear at 1580 and 1620 cm^{-1}. These may be attributed to C=C and/or C=N stretching (C=C stretching, 1590–1670 cm^{-1} and C=N stretching, 1580–1620 cm^{-1}). At 450 °C, the nitrile group has almost disap-

Table 4
Elemental analysis of copolymers and their product after thermal treatment

CHN results	R3	R3′	R6	R6′
% C	79.3	71.7	76.9	76.3
% H	7.0	3.6	7.8	6.3
% N	12.2	6.8	15.8	13.4
% O	1.5	17.9	0.0	4.0

R3′ = residue at 450 °C; R6′ = copolymer after thermal treatment at 100 °C during 5 days CHN, elemental analysis, error = 0.1%.

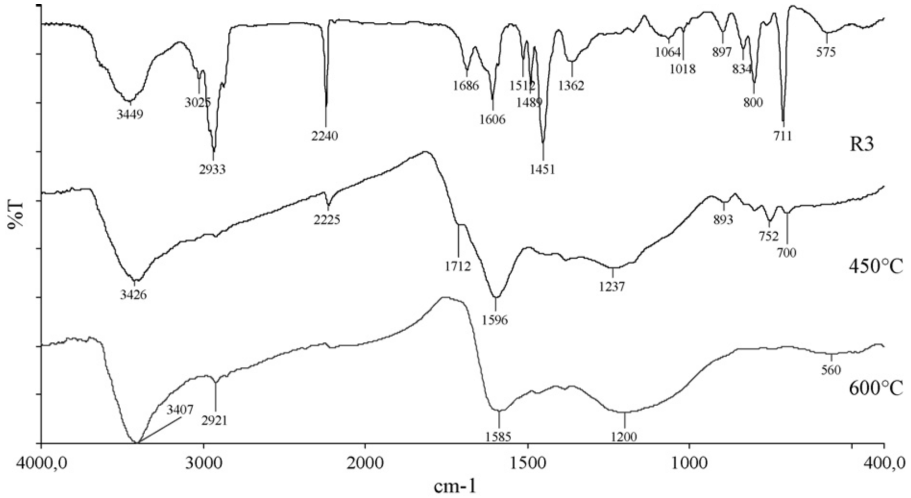

Fig. 4. FTIR spectra of the R3 copolymer and its residues obtained at 450 and 600 °C.

peared and the bands for C=C and/or C=N are fully developed. From the CHN analysis, the composition of the residue does not begin to change until 275 °C. This implies that AN segments cyclization process occurs without loss of any material. As also discussed by Xue and Wilkie [34], from the TGA data no weight loss is noted until 290 °C.

The R6 copolymer was submitted to the constant temperature (around 100 °C) for a long time (5 days) under usual atmosphere. After this treatment, the material (R6′) was analyzed by FTIR (Fig. 5) and elemental analysis (Table 4). The R6′ spectrum displays the band at 1685 cm^{-1}, which is related to C=C vibration of the enamine. The band related to imine group was observed on the R6 spectrum (C=N, at 1634 cm^{-1}). Under heating, the enamine/imine equilibrium was displaced to the formation of the enamine structure, which is related to the appearance of a broad band at 1585 cm^{-1} [16,19]. The significant increase of the cyclization implies the intensity reduction of CN absorption [18]. It was observed another change in FTIR spectra, which was the presence of the characteristic C=O band at 1711 cm^{-1}. This absorption could be attributed to the thermooxidation process of nitrile groups. One note that CHN values indicate the increasing of the oxygen content for R6′, what confirms the occurrence of oxidative process during the resins drying. Therefore, the oxygen content of intermediate residue of R3 resin (at 450 °C) could be attributed to this earlier oxidation at the oven (drying process). Additionally, the appearance of C=O absorption displayed in the FTIR spectra could also be explained by this previous drying.

Comparing TGA curves of R3 and R5 resins to the porosity characteristics (Table 2), it is possible to note that the porosity did not have a significant role on the thermal behavior. The difference between T_{dm2} values of these copolymers is 16 °C. The same behavior was observed for R1 and R2 copolymers (15 °C, difference between their T_{dm2}). On the other hand, the R3 and R6 resins have shown large difference between their T_{dm2} values (42 °C). As the crosslinking degree of these materials is the same, it seems that the AN content incorporated to the copolymer could explain this result, namely $N_{R3} = 12.2$ and $N_{R6} = 15.8$ (Table 4). These results evidence that the ACT/TOL diluent sys-

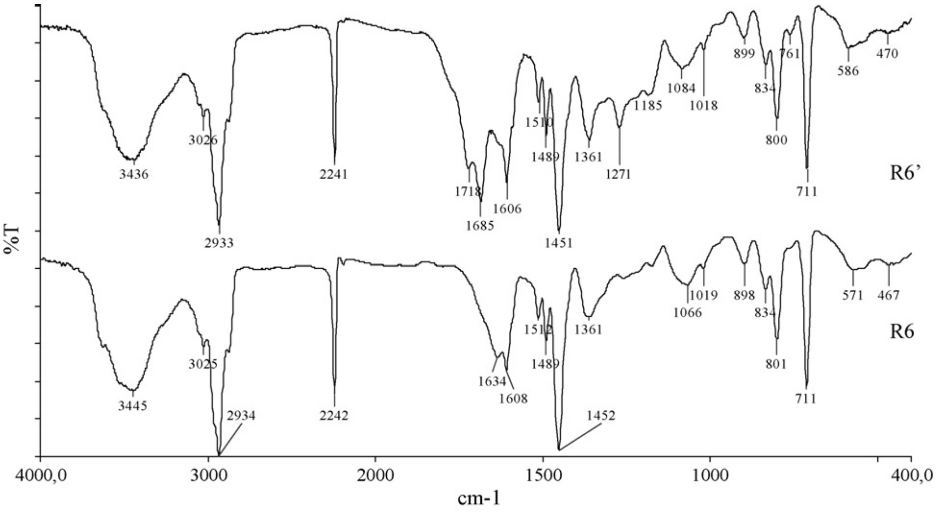

Fig. 5. FTIR spectra of the R6 copolymer and the product (R6′) obtained after thermal treatment at 100 °C for 5 days.

tem is better than ANI for improving the AN incorporation. TGA curve of R6 resin clearly shows that the first mass loss is less remarkable than the others. In addition, the second stage of thermal degradation was depicted at higher temperature compared to the others.

4. Conclusions

The TG-DTG results up to 800 °C and IR-spectroscopic data provided a picture of the multi-stage thermal decomposition processes of copolymers based on acrylonitrile crosslinked with divinylbenzene. These processes could be attributed to the removal of moisture from the polymer matrices, the primary crosslinking of the chains, their aromatization and condensation due to the crosslinking of polynuclear structure.

Acknowledgements

We are grateful for the financial support of CAPES, FAPERJ and CNPq. We thank the follow companies: Metacril do Brasil for reagents donation and Nitriflex for elemental analyses and monomers donation.

References

[1] L.C. Santa Maria, M.C.V. Amorim, M.R.M.P. Aguiar, P.I.C. Guimarães, M.A.S. Costa, A.P. Aguiar, P.R. Rezende, M.S. Carvalho, F.G. Barbosa, J.M. Andrade, R.C.C. Ribeiro, React. Funct. Polym. 49 (2001) 133–143.
[2] V. Smigol, F. Svec, J.M.J. Fréchet, Macromolecules 26 (1993) 5615–5620.
[3] R.A. Beauvais, S.D. Alexandratos, React. Funct. Polym. 36 (1998) 113–123.
[4] O. Okay, Prog. Polym. Sci. 25 (2000) 711–779.
[5] E.C. Riqueza, A.P. Aguiar, L.C. Santa Maria, M.R.M.P. Aguiar, Polym. Bull. 48 (2002) 407–414.
[6] E.C. Riqueza, L.C. Santa Maria, M.R.M.P. Aguiar, A.P. Aguiar, Mater. Lett. 58 (2004) 502–506.
[7] E.C. Riqueza, A.P. Aguiar, L.C. Santa Maria, M.R.M.P. Aguiar, Polym. Bull. 55 (2005) 31–40.
[8] N.T. Kartel, J. Therm. Anal. Calorim. 62 (2000) 499–507.
[9] A. Trochimczuk, J. Pielichowski, B.N. Kolarz, Eur. Polym. J. 26 (1990) 959–961.
[10] A. Trochimczuk, B.N. Kolarz, Polym. Commun. 30 (1989) 369–371.
[11] B.N. Jang, C.A. Wilkie, Polymer 46 (2005) 9702–9713.
[12] Z. Bashir, Carbon 29 (1991) 1081–1090.
[13] M. Suzuki, A.A. Wilkie, Polym. Degrad. Stab. 47 (1995) 217–221.
[14] W. Chengwang, D. Qingyi, H. Shaohui, Thermochem. Acta 331 (1999) 61–65.
[15] I. Bunia, C.N. Cascaval, D. Rosu, C. Ciobanu, M. Popa, Polym. Degrad. Stab. 70 (2000) 205–215.
[16] B. Mailhot, J.L. Gardette, Polym. Degrad. Stab. 44 (1994) 223–235.
[17] S. Dalton, F. Heatley, P.M. Budd, Polymer 40 (1999) 5531–5543.
[18] G.X. Zhao, B.J. Chen, S.A. Qian, J. Anal. Appl. Pyrolysis 23 (1992) 87–97.
[19] N. Grassie, R. McGuchan, Eur. Polym. J. 8 (1972) 865–878.
[20] T.J. Xue, M.A. McKinney, C.A. Wilkie, Polym. Degrad. Stab. 58 (1997) 193–202.
[21] L.H. Peebles, P. Peyser, W. Snow, W.C. Peters, Carbon 28 (1990) 707–715.
[22] G.H. Olivé, S. Olivé, Adv. Polym. Sci. 51 (1983) 1–60.
[23] A.A. Berlin, A.M. Dubinskaya, Y.S. Moshkovski, Polym. Sci. USSR 6 (1966) 2145–2151.
[24] J. Ferguson, B. Mahapatro, Fibre Sci. Tech. 9 (1976) 161–168.
[25] H.H.G. Jellinek, A. Das, J. Polym. Sci., Polym. Chem. 16 (1978) 2715–2719.
[26] M. Wojaczynska, B.N. Kolarz, J. Chromatogr. 358 (1986) 129–136.
[27] D.R. Lide, Handbook of Chemistry and Physics, 78th ed., CRC, New York, 1997.
[28] O. Okay, Angew. Makromol. Chem. 157 (1988) 1–13.
[29] J. Brandrup, E.H. Immergut, Polymer Handbook, second ed., John Wiley and Sons, New York, 1974.
[30] I.C. Poinescu, M. Barbu, C. Vlad, S. Dragan, Eur. Polym. J. 33 (1997) 153–156.
[31] C.M. Hansen, J. Paint Technol. 39 (1967) 104–111.
[32] J.B. Lambert, H.F. Shurvell, D.A. Lightner, R.G. Cooks, Organic Structural Spectroscopy, Prentice-Hall, New Jersey, 1998.
[33] M.M. Coleman, R.J. Petcavich, J. Polym. Sci. Polym. Phys. Ed. 16 (1978) 821.
[34] T.J. Xue, C.A. Wilkie, Polym. Degrad. Stab. 56 (1997) 109–113.